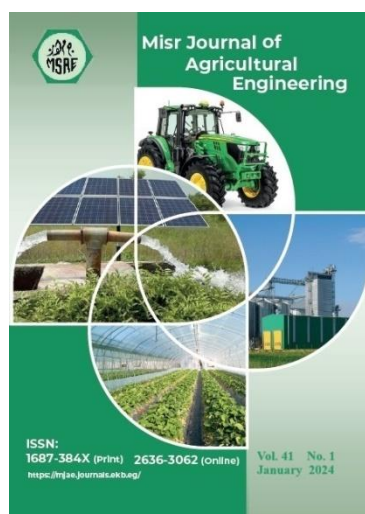


EFFECT OF SOME ENGINEERING PARAMETERS OF IMPACT SPRINKLER ON PERFORMANCE RATE AND DROPLET KINETIC ENERGY

Sally A. Amin¹, Mahmoud M. Hegazi², Abdelhameed T. Gaballa³ and
Khaled. F.El Bagoury⁴

1. PhD Stud., Soil and Water Conservation Dept., Desert Res. Center Cairo, Egypt.
2. Prof. Emeritus, Ag. Eng. Dept., Fac. of Ag., Ain Shams U., Cairo, Egypt.
3. Prof. Emeritus, Soil and Water Conservation Dept., Desert Res. Center, Cairo, Egypt.
4. Prof., Ag. Eng. Dept., Fac. of Ag., Ain Shams U., Cairo, Egypt.

* E-mail: eng_sally_3sy@yahoo.com



© Misr J. Ag. Eng. (MJAE)

Keywords:

Sprinkler; nozzles; kinetic energy; precipitation rate; droplet size.

ABSTRACT

This Research aims to obtain appropriate management for Impact sprinklers to overcome the problem of soil damage due to droplets' kinetic energy. Nozzle pressure and diameter had a major influence on droplet size which highly affects the droplet kinetic energy. Experiments were conducted at the National Irrigation Laboratory of Agricultural Engineering Research Institute (AEnRI), Dokki, Giza, Egypt was chosen to represent the engineering data of the selected impact sprinkler, riser and operating pressure. Two different nozzle diameters 3.2 mm and 3.9 mm were examined in this work at three different pressures range: 175 kPa, 200 k Pa and 225 kPa

Then we found the results as follow:

- *Precipitation rates at pressure 225 kPa are the most regular rates, followed by pressure 200 kPa followed by pressure 175 kPa for the two tested nozzles.*
- *Droplet Kinetic energy at the end of the wet diameter at nozzle diameter 3.2 mm is 26.83 J (10)⁻³, 23.9 J (10)⁻³ and 18.3 J (10)⁻³ at pressure 175 kPa, 200kPa, and 225kPa respectively, and at nozzle diameter 3.9 mm is 37.7 J 10⁻³, 35.78 J (10)⁻³ and 27.82 J (10)⁻³ at pressure 175 kPa, 200kPa, and 225kPa respectively.*

INTRODUCTION

Water is the scarcest resource; it is unnecessary to emphasize the value of using it wisely in the agriculture industry to support agricultural expansion and slow down environmental damage. The effectiveness of using sprinkler irrigation for new land development points the way forward to a larger role in the development of future land reclamation projects. On-farm productivity must be increased through improved water management practices and other production aspects, according to **Darko et al. (2017)**.

Soil types are categorized as arid because of the climate and parent soil. These soils were characterized by a finer texture, a weak structure, a high proportion of calcium carbonate, a

low level of organic matter, and a saline soil (Muhaimed et al., 2014). Despite being one of the most popular watering methods, sprinklers have downsides in the form of soil crusting, runoff, and injury to plant parts, especially during the first stage of growth, (Zhang and Zhu, 2017). Additionally, to minimize detrimental impacts on the soil's physical properties, the sprinkler irrigation system needs to be operated with expertise. This is done by adjusting the sprinkler nozzle and operating pressure to change the size of the sprinkler droplets and prevent soil crusting. Sprinkler droplet energy weakens the surface soil structure and linearly increases the penetration resistance (Baumhardt et al., 2004). A larger droplet sprinkler causes compaction, lowers aggregate stability, slows down soil infiltration, and raises soil bulk density (Santos et al., 2003). According to Sheikhesmaeili et al. (2016), increasing operating pressure from 0.45 MPa to 0.5 MPa is expected to result in an 18% rise in energy costs; consequently, slightly lowering operating pressure can drastically lower operating costs. It is typically observed that the kinetic energy of individual water drops striking a bare soil surface causes the rate of water infiltration to drastically decrease because of the creation of a soil surf. Seasonal runoff and soil erosion can be significantly impacted by kinetic energy that is delivered to the soil during center-pivot sprinkler irrigation prior to crop canopy establishment (King and Bjorneberg, 2010). Compared to the spray plate sprinklers applied to center pivots, the big gun sprinkler shows a milder precipitation process, but the water application lasts longer and carries more kinetic energy, reaching 2- 4 times for the same amount of water. The infiltration rate of each location decreases linearly along with an increase in distance to the travel lane, and the infiltration rate decreases to approximately 20 mm/h at the end of the spraying area (Maosheng et al., 2018). Stillmunkes and James (1982) show that the impact energy increases slowly for droplet larger than 6 mm Wang et al. (2020) stated that splash erosion rate of soil increase by increasing droplet kinetic energy, soil erosion starting to begin at droplet kinetic energy $0.3 \text{ J } (10^{-1})$ of amount 50 g.m^2 this soil erosion tripled to 150 g.m^2 at droplet kinetic energy $0.4 \text{ J } (10^{-1})$, and reach a high level of amount 300 g.m^2 at droplet kinetic energy $0.9 \text{ J } (10^{-1})$. Lehrsch and Kincaid (2001) stated that the increase in steady-state infiltration rate from -40 to -20 nun at droplet energy $1 \text{ J } (10^{-3})$ was $6.8 \text{ nun h}''$, nearly 45% greater than the increase of droplet energy at $7 \text{ J } (10^{-3})$

Objectives of the research: The research aimed to study the kinetic energy and precipitation rates emitted by impact sprinklers in the absence of wind (indoor conditions), to reduce the sprinkler base pressure to the limit that maintains acceptable droplet size, diameter, and kinetic energy. Maps of specific coefficients of precipitation rates are presented as a methodological contribution to decision- making in sprinkler system design and management.

MATERIALS AND METHODS

Materials.

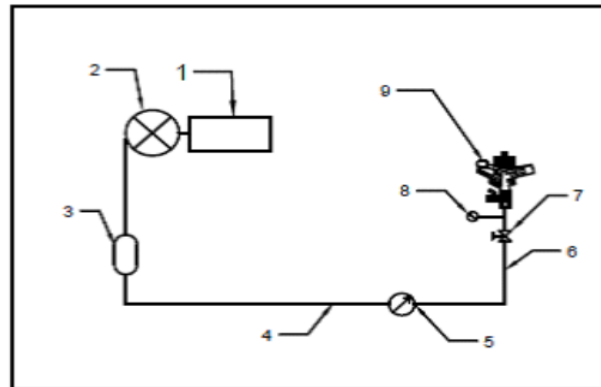
Location

Laboratory experiments were carried out at the National Irrigation Laboratory of Agricultural Engineering Research Institute (AEnRI), Dokki, Giza, Egypt,

Layout of the experimental irrigation line

Laboratory experiment components was shown in Fig. (1). The main point of this research was to study the effect of engineering factors (nozzle diameter and operating pressure) on the precipitation rate and droplet kinetic energy at the beginning, middle, and end of the wet radii

of the sprinkler application to save energy and prevent the destruction of the surface layer of the soil.



- | | | |
|-----------------|------------------|---------------------|
| 1- Water source | 2- Pump | 3- Disc filter |
| 4- Steel pipe | 5- Flow meter | 6- Sprinkler riser |
| 7- Ball valve | 8- Pressure gage | 9- Impact sprinkler |

Fig. (1): The layout of the experimental irrigation line, and the description of this equipment is listed below

Control head as using of National Irrigation Laboratory:

- Water source: Tank made of concrete 8 m³ volume.
- Pumping unit: Its specifications are shown in Table (1).

Table 1: Pumping unit specification:

Type	centrifugal pump NT 80 – 400	Inlet diameter	4”
Capacity	100 m ³ /h	Outlet diameter	3”
KW	30	Man. Head	55 m
W2 – No	0410294/5	RPM	1450

- Disc filter: 3", 120 mesh, 130 microns.
- Steel pipe: 1 1/2" diameter.
- Flow meter: 1 1/2" diameter, maximum discharge was 12 m³/h.
- Ball valve: 3/4", UPVC.
- Pressure gauge: 1000 k Pa

The riser:

Sprinkler riser: 1 m height, it is made of UPVC pipe, ISO 9001, 1/2" inlet diameter, threaded pipe

The sprinkler:

Impact sprinkler

- Rotation: part circle / full circle.
- Impact 1/2" inlet diameter, one circular nozzle.
- Made of plastic.
- Angle: 30°.

The sprinkler is shown in Figure 2

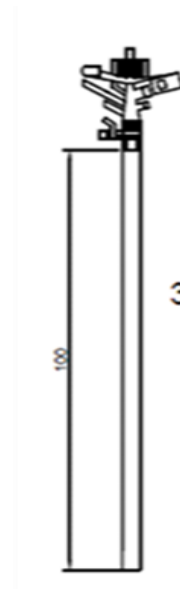


Fig.(2): AQ-22 PC-AG 1/2 inches sprinkler

Sprinkler performance

relation between pressure, flow rate and wet diameter from the sprinkler catalog is shown in figure 3



Nozzle (mm)	Pressure		Coverage Diameter		Discharge Rate	
	kg/cm ²	Psi	mtr.	ft.	LPM	GPM
2.5	2.0	28.44	21.0	68.88	6.10	23.09
	2.5	35.55	22.0	72.16	6.80	25.74
	3.0	42.66	21.6	70.85	7.40	28.02
	3.5	49.77	22.6	74.13	8.00	30.29
2.9	4.0	56.88	22.6	74.13	8.55	32.37
	2.0	28.44	23.0	75.44	7.60	28.76
	2.5	35.55	23.0	75.44	8.50	32.18
	3.0	42.66	23.0	75.44	9.30	35.21
3.2	3.5	49.77	23.0	75.44	10.10	38.24
	4.0	56.88	23.0	75.44	10.75	40.70
	2.0	28.44	22.0	72.16	9.40	35.59
	2.5	35.55	23.0	75.44	10.50	39.75
*3.5	3.0	42.66	23.0	75.44	11.55	43.73
	3.5	49.77	23.5	77.08	12.45	47.14
	4.0	56.88	24.0	78.72	13.30	50.35
	2.0	28.44	22.0	72.16	11.70	44.30
*3.5	2.5	35.55	23.0	75.44	13.10	49.59
	3.0	42.66	24.0	78.72	14.30	54.14
	3.5	49.77	25.0	82.00	15.40	58.30
	4.0	56.88	26.0	85.28	16.40	62.09

*Performance is based on ideal conditions of Temperature, wind velocity and Humidity.

Fig. (3): sprinkler performance

Nozzles

Two circular nozzles of diameters 3.2 mm and 3.9 mm were used in the experiment as shown in Figures 4 and 5



Fig. (4):Nozzle 1; its shape is circular, and its diameter equals 3.2 mm

Fig. (5): Nozzle 2; its shape is circular, and its diameter equals 3.9 mm

The water collectors:

Water collectors are plastic cylindrical cans with inner diameter 70 mm and 200 mm in height, were arranged under the impact of the sprinkler to measure the volume of water then measure the precipitation rate

Computer programs:

Software's Surfer10, Version 2.4, is a full-function 3D visualization, contouring and surface modeling package that runs under Microsoft Windows. Surfer is used extensively for terrain modeling, landscape visualization, surface analysis, contour mapping, 3D surface mapping, gridding, volumetric, and more. This program shows the precipitation rate pattern of sprinkler under three different operating pressure using two different discharges of two nozzles. Software's Surfer10 is designed to simulate and graph, in three dimensions, surfer can measure from either a single sprinkler head test or single lateral line test. The surfer program is an interactive IBM-PC program written in Microsoft Professional Basic (v. 7) language. (Allen, 1992).

Methods

Droplet diameter:

Droplet size diameters were measured, at three different distances from the sprinkler; at the beginning, at the middle and at the end of the wet radius.

1. The droplet diameter at different operating pressure was measured by using filter paper. When the droplet falls on the filter paper, it made a small circular in the paper. We can be measuring the droplet diameter by using a small ruler (Hall, 1970).

Droplet volume

The volume of the droplet was calculated by means of droplet density and mass

$$V = M / \rho \dots\dots\dots (1)$$

Where:

- V=Droplet volume, cm³
- M= Droplet mass, g
- ρ=water density, g /cm³

Kinetic energy

It was determined according to (Cengel and Cimbala, 2009) stated that the kinetic energy of sprinkler droplets is based on the following equation:

$$K_e = 0.5 m v^2 \dots\dots\dots (2)$$

Where:

- K_e = Kinetic energy/droplet, (joule)
- m = droplet mass, (kg_m)
- v = droplet velocity, (m/s)

The mass of the droplet was calculated by equation (1), and volume by equation (3)

- The actual droplet size volume can be determined mathematically as a function of droplet diameter referring to the following equation

$$\text{Volume of water droplet} = \frac{4}{3} \pi \left(\frac{d}{2}\right)^3 \dots\dots\dots (3)$$

- v = Droplet volume, cm^3
- d =Droplet diameter, cm

Droplet velocity calculations:

According to (Nolte, 2018)

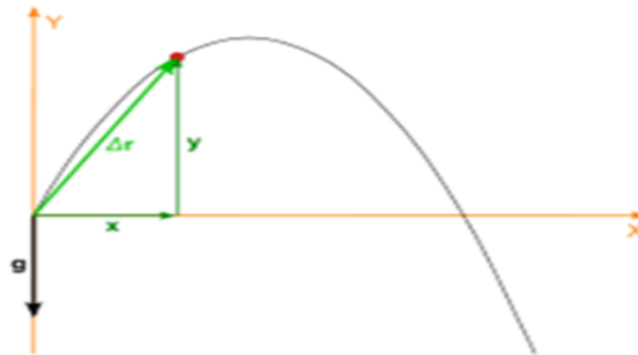


Fig. (6): Parabolic water motion

$$y = -\frac{g}{2v_0^2 \cos^2 \alpha} x^2 + \tan \alpha \cdot x \dots\dots\dots(4)$$

$$x = v_0 \cos \alpha t \dots\dots\dots(5)$$

$$v_y = v_0 \sin \alpha - gt \dots\dots\dots(6)$$

$$v_x = v_0 \cos \alpha \dots\dots\dots (7)$$

$$v_A = \sqrt{v_{x_A}^2 + v_{y_A}^2} \dots\dots (8)$$

Where:

X = Position component in the horizontal direction, m

Y = Position component in the vertical direction, m

t = time, s

$V_x = dx/dt$ = horizontal component of velocity V , m/s

$V_y = dy/dt$ vertical component of velocity V , m/s

α = Trajectory angle of sprinkler = 25°

g =Gravity acceleration, 9.81 m/s^2

Nozzles Discharge:

Measure the water collected from the sprinkler nozzle using a 1000 ml graduated cylinder.

Determine the flow rate from the following equation:

(Melvyn, 1983 and Sayed, 2016):-

$$Q=V/T\dots\dots\dots (9)$$

Where:

Q= discharge, L/s

V= collected water volume, L

T= time of collecting water, s

Precipitation rate:

The precipitation rate of the sprinkler was calculated by the following formula (James, 1988):-

$$pr = k \frac{Q}{a} \dots \dots \dots (10)$$

Where:

Pr = The precipitation rate in mm /h.

Q = The flow rate of the sprinkler in m³/h.

a = The wet area of sprinkler in m².

K = Unit constant =1000 (converts meters to millimeters).

Plastic catch cans of 70 mm diameter, 200 mm height were located under impact sprinkler of range 15 m, in a quarter circle. The catch cans were distributed according to (ASAE, 2001) as it is presented in Fig. (7).

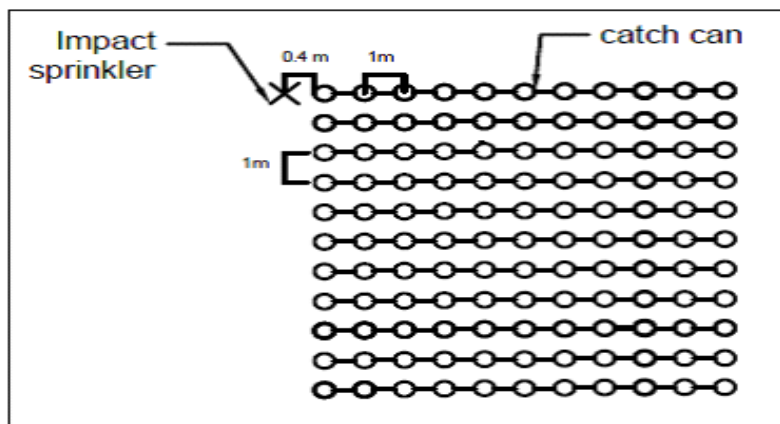


Fig. (7): Arrangement of catch cans for impact sprinkler.

Experimental layout and parameter

Measuring precipitation rates and droplet’s kinetic energy at the beginning ,middle and the end of the wet radius of the impact sprinkler:

1- Two different nozzle diameters

a- 3.2 mm

b- 3.9 mm

2- Three different pressures

a- 175 kPa

b- 200 kPa

c- 225 kPa

RESULTS AND DISCUSSION

Droplet diameters and sprinkler's wet radii at the three different pressure range

Wet area radii for each nozzle 3.2 mm and 3.9 mm diameter under the three different working pressure 175, 200, and 225 kPa were measured and droplet diameter at the beginning, middle, and end of the wet area radius were measured as shown in table (2). These data reveal that droplet diameter increases as the nozzle diameter increases under all working pressure. However, droplet diameter decreases as the working pressure increases. Likewise, droplet diameter increases from the beginning of the wet radius to the end of it. This reveals that the soil surface at the end of the sprinkler impact radius and the larger nozzle diameter will be more vulnerable to the effect of the kinetic energy

Table 2: the wet area radii and the drop diameters of the two nozzles

Factors	175 kPa.		200 kPa.		225 kPa.	
	Nozzle diameter, mm		Nozzle diameter, mm		Nozzle diameter, mm	
	3.2	3.9	3.2	3.9	3.2	3.9
Sprinkler wet radius, m	9	9.5	11	12	12	12.8
Droplet diameter at the beginning of the wet radius, mm	3	4	2	3	1	2
Droplet diameter at the middle of the wet radius, mm	6	7	5	6	4	5
Droplet diameter at the end of the wet radius, mm	10	11	9	10	8	9

Table 3: Shows Droplet Velocity at the beginning, middle and the end of the wet area radii of the two nozzles diameters 3.2 mm and 3.9 mm under the three different working pressure at 175,200,225 kPa.

Factors	175 kPa.		200 kPa.		225 kPa.	
	Nozzle diameter, mm		Nozzle diameter, mm		Nozzle diameter, mm	
	3.2	3.9	3.2	3.9	3.2	3.9
Droplet Velocity at the beginning of the wet radius, m/s	4.13	4.15	4.21	4.24	4.33	4.40
Droplet Velocity at the middle of the wet radius, m/s	7.1	7.3	7.9	8.2	8.3	8.5
Droplet Velocity at the end of the wet radius, m/s	10.13	10.40	11.2	11.70	11.7	12.07

Initial velocity (v_0) was calculated from equation 4 (Path equation), then time was calculated from equation 5, v_y and v_x was calculated by using equation 6. Finally droplet velocity was calculated by equation 8

Table 4: volume of droplet, mass and its kinetic energy at the beginning of the wet area radius at the three different working pressure

Factors	Pressure					
	175 kPa		200 kPa.		225 kPa.	
	At Nozzle diameter, 3.2 mm	At Nozzle diameter, 3.9 mm	At Nozzle diameter, 3.2 mm	At Nozzle diameter, 3.9 mm	At Nozzle diameter, 3.2 mm	At Nozzle diameter, 3.9 mm
Volume of droplet, cm ³	0.01413	0.03349	0.00418	0.01413	0.00052	0.00418
Mass of droplet, gm	0.01413	0.03349	0.00418	0.01413	0.00052	0.00418
Mass of droplet, kg	1.41E-5	3.35E-5	4.19E-6	1.41E-5	5.23E-7	4.19E-6
Velocity of droplet, m/s	4.1342	4.13422	4.1342	4.1342	4.1342	4.1342
K.E,j	0.00012	0.00028	3.58E-5	0.00012	4.47E-6	3.58E-5
K.E, j(10 ⁻³)	0.121	0.286	0.0358	0.121	0.004	0.036

Table 5: volume of droplet, mass and its kinetic energy at the middle of the wet area radius at the three different working pressure 175, 200, and 225 kPa

Factors	Pressure					
	175 kPa		200 kPa.		225 kPa.	
	At Nozzle diameter, 3.2 mm	At Nozzle diameter, 3.9 mm	At Nozzle diameter, 3.2 mm	At Nozzle diameter, 3.9 mm	At Nozzle diameter, 3.2 mm	At Nozzle diameter, 3.9 mm
Volume of droplet, cm ³	0.11304	0.17950	0.06541	0.1130	0.03349	0.06541
Mass of droplet, gm	0.11304	0.17950	0.06541	0.1130	0.03349	0.06541
Mass of droplet, kg	0.00011	0.00018	6.54E-5	0.00011	3.35E-5	6.54E-5
Velocity of droplet,m/s	7.161	7.357	7.916	8.268	8.268	8.539
K.E,j	0.00289	0.00485	0.00205	0.0039	0.00115	0.00239
K.E, j(10 ⁻³)	2.898	4.858	2.049	3.864	1.145	2.385

Table 6: volume of droplet, mass and its kinetic energy at the end of the wet area radius at the three different working pressure 175, 200, and 225 kPa

Factors	Pressure					
	175 kPa		200 kPa.		225 kPa.	
	At Nozzle diameter, 3.2 mm	At Nozzle diameter, 3.9 mm	At Nozzle diameter, 3.2 mm	At Nozzle diameter, 3.9 mm	At Nozzle diameter, 3.2mm	At Nozzle diameter, 3.9 mm
Volume of droplet, cm³	0.52333	0.69656	0.38151	0.5233	0.26794	0.38151
Mass of droplet, gm	0.52333	0.69656	0.38151	0.5233	0.26795	0.38151
Mass of droplet, kg	0.00052	0.00070	0.00038	0.00052	0.00027	0.00038
Velocity of droplet, m/s	10.1267	10.4042	11.1955	11.693	11.6933	12.0768
K.E, j	0.0268	0.0377	0.02390	0.0239	0.03577	0.01831
K.E, j(10⁻³)	26.8341	37.7004	23.9092	35.779	18.3188	27.8216

Kinetic energy at different distances from the nozzle

Figures (8a) and (8b) display the kinetic energy intensity distribution of each nozzle under different working pressure levels. According to Figure 8 a, the maximum kinetic energy intensity of the 3.2 mm nozzle at pressure 175 kPa ,at the end of the wet radius , and it is equals to $26.83 \text{ j}(10^{-3})$, that is contributed to the droplet diameter and velocity , followed by kinetic energy of water droplet at pressure 200 kPa , followed by kinetic energy of water droplet at pressure 225 kPa, which equal $23.9 \text{ j}(10^{-3})$ and $18.3 \text{ j}(10^{-3})$ respectively. According to Figure (8b), the maximum kinetic energy intensity of the 3.2 mm nozzle at pressure 175 kPa ,at the end of the wet radius , and it is equals to $37.7 \text{ j}(10^{-3})$, that is contributed to the droplet diameter and velocity , followed by kinetic energy of water droplet at pressure 200 kPa,, , followed by kinetic energy of water droplet at pressure 200 and 225 kPa, which equal $35.78 \text{ j}(10^{-3})$ and $27.82 \text{ j}(10^{-3})$ respectively. In general, the 3.9 mm nozzle causes higher levels of kinetic that cause detrimental effect on soil erosion and soil infiltration rate according to **Yanjun Wang et al. (2020) , Lehrsch and Kincaid (2001)**

Sprinkler precipitation

Figure (9 a) and (9 b) show the radial water distribution of two circular nozzles with different outlet diameters of 3.2mm and 3.9mm diameter the order of $D2 > D1$ under different working pressure levels. It can be observed that the water intensity (precipitation rate) increased by increasing the nozzle diameter and the working pressure

Topographic maps of moisture distribution under the impact sprinkler

Fig. (10,11) Represent the precipitation rates pattern for the impact sprinkler of the two circular nozzles with different outlet diameters (3.2mm, 3.9mm) under pressure 175 kPa, surfer maps reveal that low precipitation rates from 2mm/ h to 16 mm/h are dominant in the wet area under the impact sprinkler that is appears as a blue color in the map where is the

sufficient precipitation rates from 32 mm/h to 47 mm/h have occupied very small area under the impact sprinkler which appears in a red color in the map. . (CU) value: 77.8 % and 79.2 % for the two nozzle diameters 3.2mm and 3.9mm respectively.

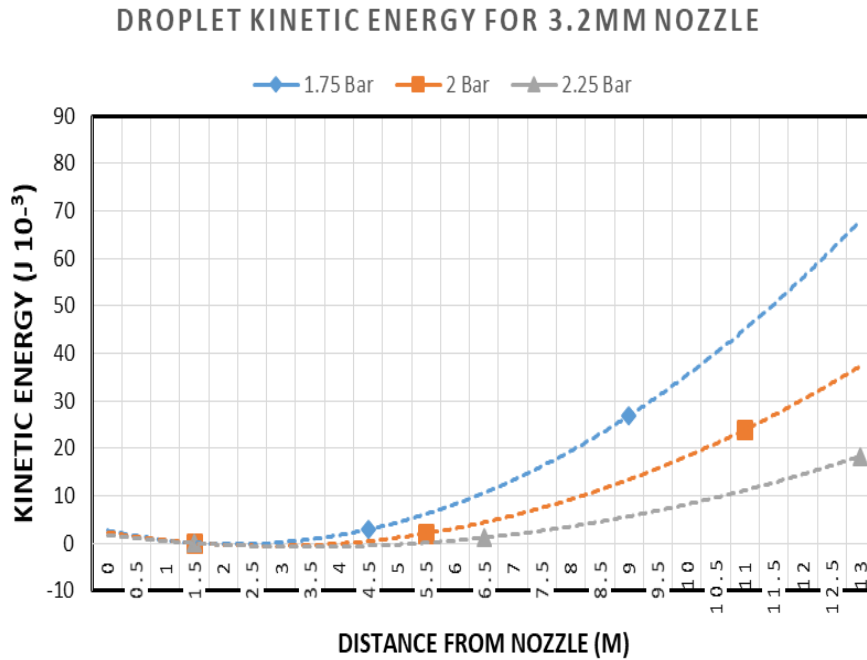


Fig. (8a): Kinetic energy intensity of two different nozzles diameter as a function of the distance from the nozzle under different working pressure levels

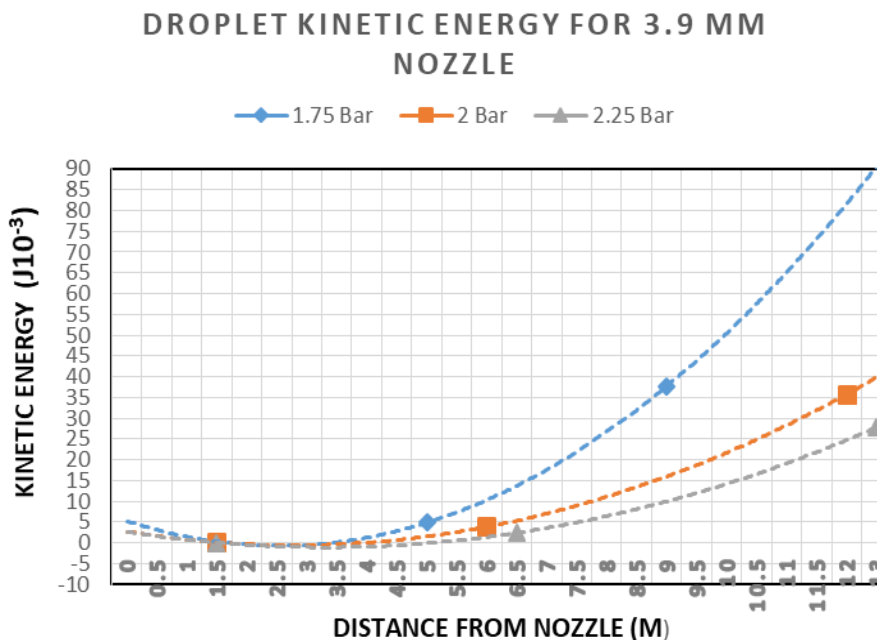


Fig. (8b): Kinetic energy intensity of two different nozzles diameter as a function of the distance from the nozzle under different working pressure levels.

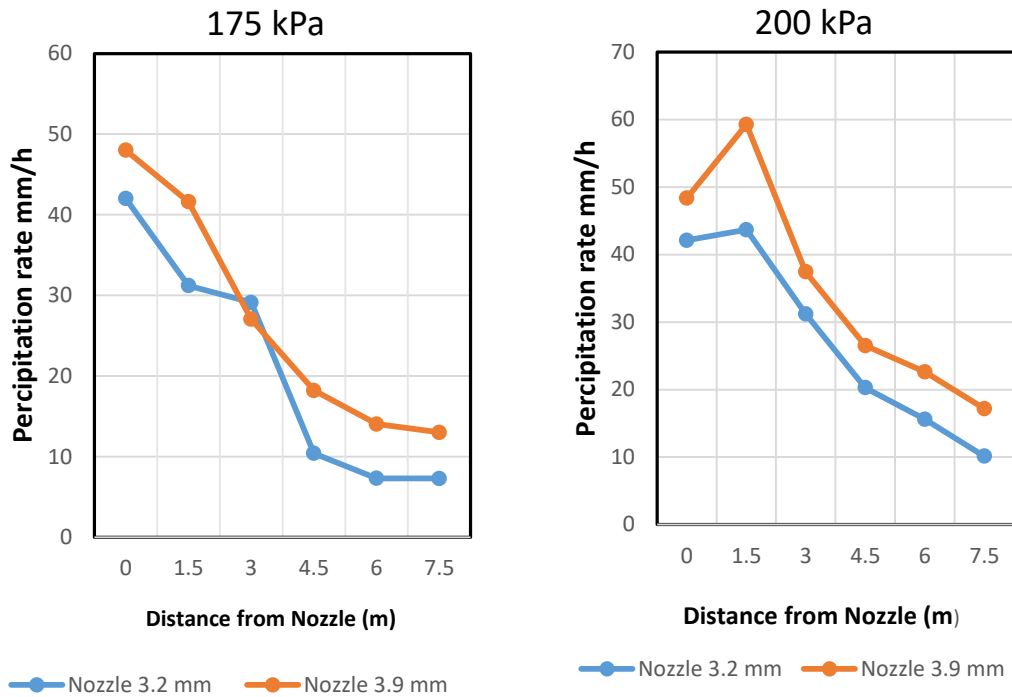


Fig. (9a): Radial water distribution of two nozzles with different outlet diameters under different working pressure levels. (175,200,225 kPa.)

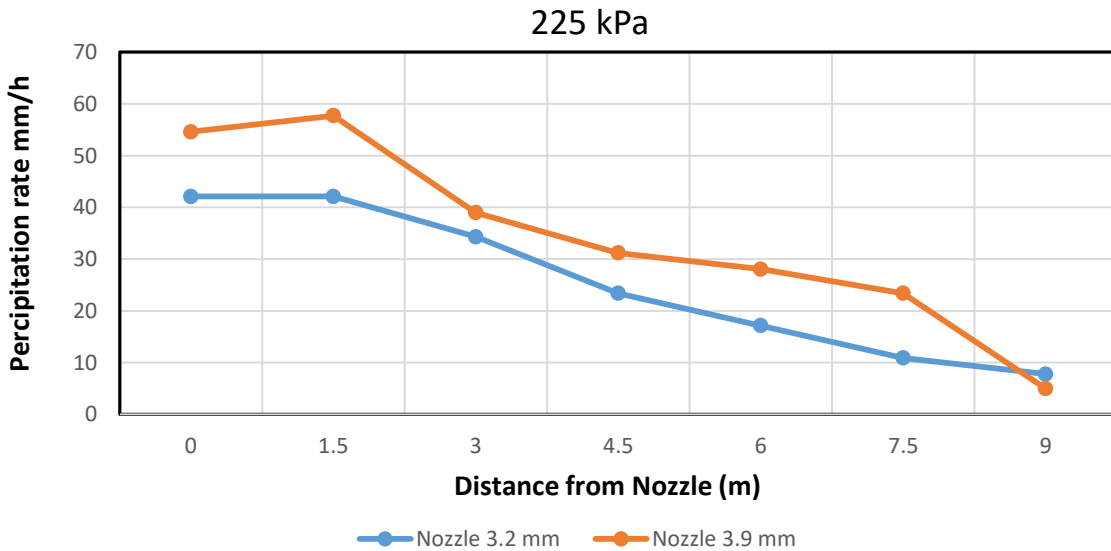


Fig. (9b): Radial water distribution of two nozzles with different outlet diameters under different working pressure levels (175,200,225 kPa.)`

Fig. (12,13) Represent the precipitation rates pattern for the impact sprinkler of the two circular nozzles with different outlet diameters (3.2mm, 3.9mm) under pressure 200 kPa, surfer maps reveal that sufficient precipitation rates from 40 mm/ h to 65mm/h are dominant in the wet area under the impact sprinkler that is appears as a red color in the map. (CU) value: 88 % and 89.2 % for the two nozzle diameters 3.2mm and 3.9mm respectively.

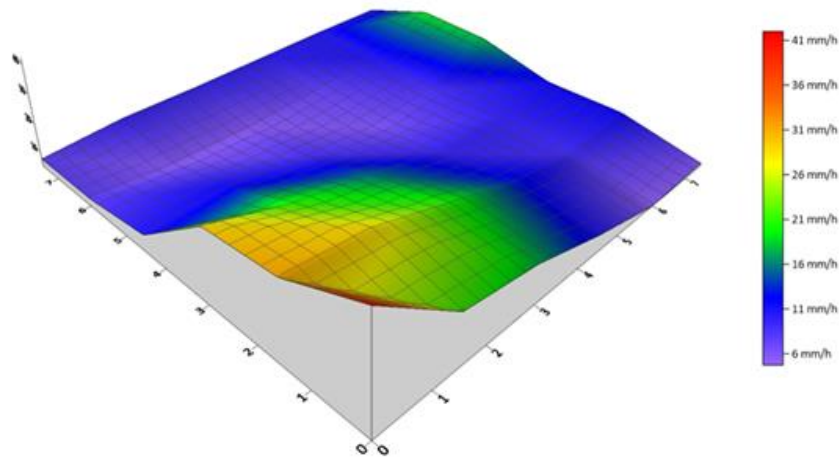


Fig. (10): Precipitation rate for nozzle diameter 3.2 mm and working pressure 175 kPa

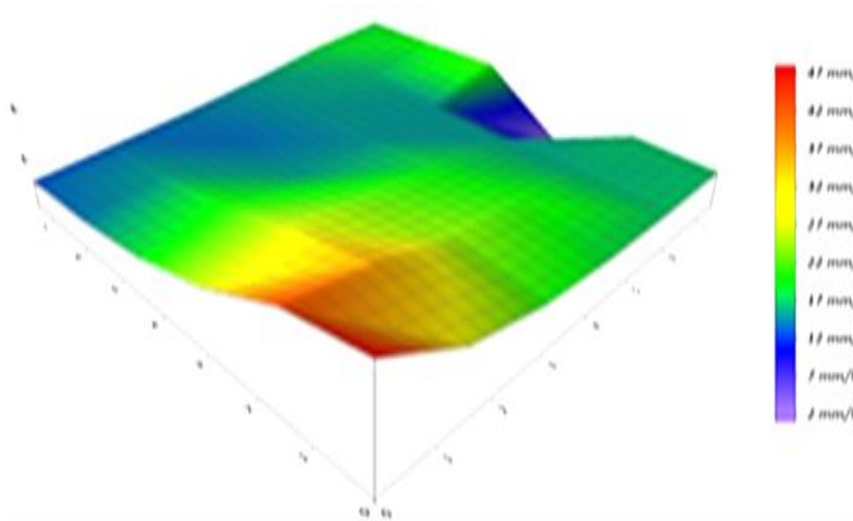


Fig. (11): Precipitation rate for nozzle diameter 3.9 mm and working pressure 175 kPa.

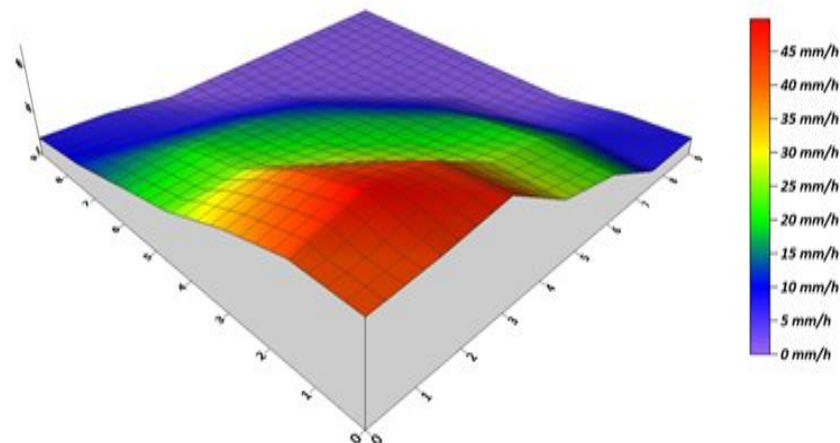


Fig.(12): Precipitation rate for nozzle diameter 3.2 mm and working pressure 200 kPa

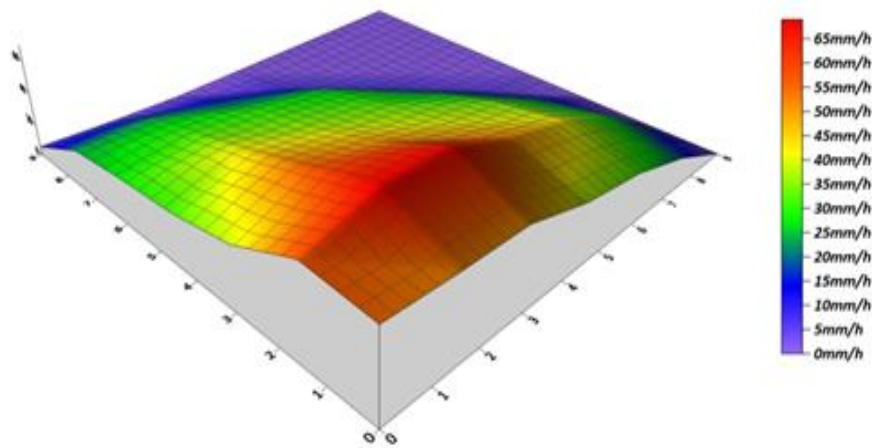


Fig. (13): Precipitation rate for nozzle diameter 3.9 mm and working pressure 200 kPa

Fig. (14,15) Represent the precipitation rates pattern for the impact sprinkler of the two circular nozzles with different outlet diameters (3.2mm, 3.9mm) under pressure 225 kPa, surfer maps reveal that sufficient precipitation rates from 40mm/h to 70 mm/h are dominant in the wet area under the impact sprinkler that is appears as a red color in the map. (CU) value: 90 % and 90.7 % for the two nozzle diameters 3.2mm and 3.9mm respectively.

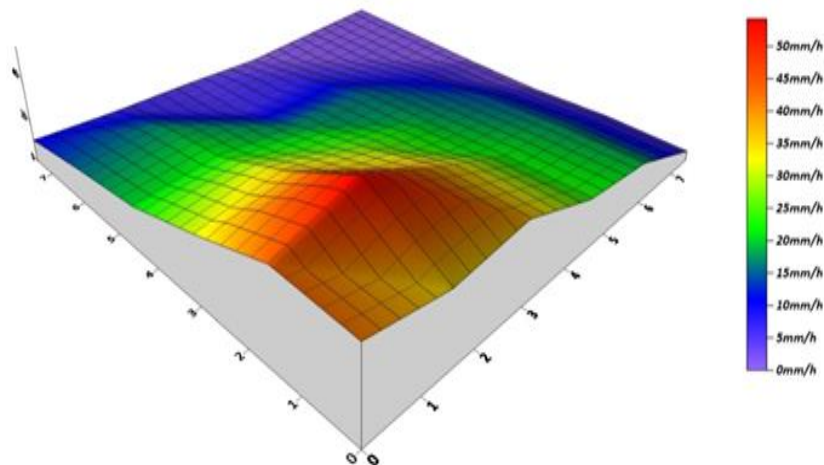


Fig. (14): Precipitation rate for nozzle diameter 3.2 mm and working pressure 225 kPa

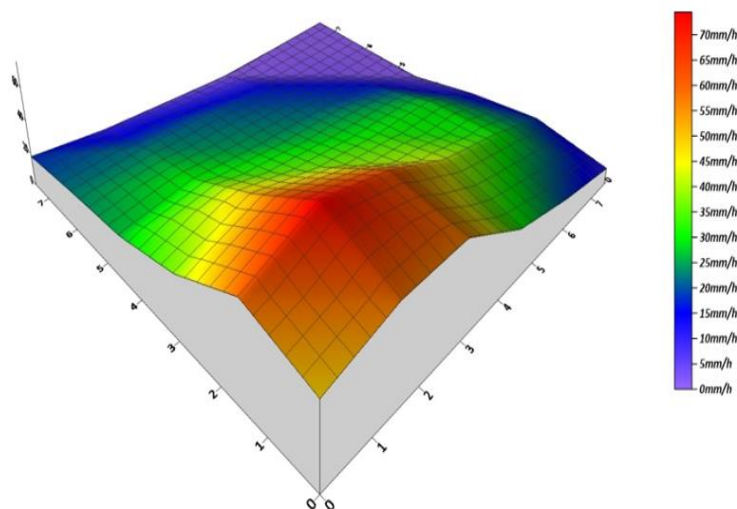


Fig. (15): Precipitation rate for nozzle diameter 3.9 mm and working pressure 225 kPa.

It can be observed that that the water intensity of the two circular nozzles with different outlet diameters (3.2mm, 3.9mm), the order of $D_2 > D_1$ under different working pressure levels increased by increasing nozzle diameter and the increasing working pressure, this is consistent with (Wang et al., 2022) .

CONCLUSION

Two nozzles' diameters 3.2mm and 3.9 mm were compared under three different working pressure 175 kPa (25.4psi), 200 kPa (29 psi), and 225 kPa (32.6 psi) on impact sprinkler. Generally, precipitation rates at pressure 225 kPa. are the most regular rates followed by pressure 200 kPa, as the Surfer maps reveal that sufficient precipitation rates from 40 mm/h to 65mm/h and from 40mm/h to 70 mm/h at pressures 200 and 225 kPa respectively are dominant in the wet area under the impact sprinkler for the two tested nozzles. At Pressure 175 kPa. low precipitation rates from 2mm/h to 16 mm/h are dominant in the wet area under the impact sprinkler, the order of $D_2 > D_1$ under different working pressure levels increased by increasing nozzle diameter and the increasing working pressure, 175 kPa is the most uneven water distribution. Moreover, there is no remarkable difference between the two pressures 200 kPa and 225 kPa. Droplet size and kinetic energy for the two nozzles (3.2mm and 3.9 mm diameter) under three working pressure (175 kPa, 200kPa and 225 kPa) were also compared, the result reveals that the 3.9 mm nozzle diameter produced the largest droplet size which equals 0.697 cm^3 and kinetic energy $37.7 \text{ kj}(10)^{-3}$ at the outer perimeter of the pattern at the lowest pressure 175 kPa and the 3.2 mm nozzle diameter produced smaller droplet size diameter at pressure 200 and 225 kPa which equal to 0.382 cm^3 and 0.269 cm^3 respectively, 3.2mm nozzle diameter also produced lower level of kinetic energy which equal 23.9 and $18.31 \text{ kj}(10)^{-3}$ at pressure 200 kPa and 225 kPa respectively, this would in fact reduce soil damage and this is in agreement with Wang et al. (2020) who stated that splash erosion rate of soil increase by increasing droplet kinetic energy, soil erosion starting to begin at droplet kinetic energy $0.3 \text{ J} (10^{-1})$ of amount 50 g.m^2 this soil erosion tripled to 150 g.m^2 at droplet kinetic energy $0.4 \text{ J} (10^{-1})$, and reach a high level of amount 300 g.m^2 at droplet kinetic energy $0.9 \text{ J} (10^{-1})$, and Lehrs and Kincaid (2001) who stated that the increase in steady-state infiltration rate from -40 to -20 nun at droplet energy $1 \text{ J} (10^{-3})$ was 6.8 nun h ", nearly 45% greater than the increase of droplet energy at $7 \text{ J} (10^{-3})$

Finally the results recommended using

- 200 kPa pressure to save power as its precipitation rate values close to 225 kPa pressure
- 3.2 mm nozzle diameter as the 3.9 mm nozzle causes higher levels of kinetic energy than the 3.2mm which cause a detrimental effect on soil physical properties.

REFERENCES

- Allen, R. G. (1992). Surfer10-software sprinkler-pattern, Version 2.4. Biological and Irrigation Engineering Department, Utah State University, Logan, Man. pp. 16.
- American Society of Association Executives (ASAE) Standard, (2001). Procedure for sprinkler testing and performance reporting. S398.1 JAN01: 880 - 882.
- Baumhardt, R. L., Unger P. W. and Dao, T. H. (2004). "Seedbed surface geometry effects on soil crusting and seedling emergence." 96(4): 1112-1117.

- Cengel, Y. A., J. M. Cimbala (2009). Fluid Mechanics, Fundamentals and Applications. 2nd Ed., McGraw-Hill.
- Darko, R. O., S. Q. Yuan, J. P. Liu, H. F. Yan and X. Y. Zhu (2017). Overview of advances in improving uniformity and water use efficiency of sprinkler irrigation. *Int. J. Agric. and Biol. Eng.*, 10(2): 1–15.
- Eigel, J. D. and I. D. Moore (1983). A simplified technique for measuring raindrop size and distribution. *Transactions of the ASAE* 26(4): 1079-1084.
- Hall, M. J. (1970). Use of the stain method in determining of the drop-size distributions of coarse liquid sprays. *Transactions of the ASAE* 13(1): 33-37.
- James, L. G. (1988). Principles of farm irrigation system design. New York: John Wiley and Sons. pp. 545.
- King, B. A., D. L. Bjorneberg (2010). Characterizing droplet kinetic energy applied by moving spray-plate center-pivot irrigation sprinklers. *American Society of Agricultural and Biological Engineers*, 53(1): 137-145.
- Lehrsch, G. A. and D. C. Kincaid (2001). Sprinkler Droplet Energy Effects on Infiltration and Near-Surface, Unsaturated Hydraulic Conductivity p. 283-286. In: D. Bosch, et al. '(ed.) preferential flow: Water movement and chemical transport in the environment. Proc. 2nd Int. Symp., Honolulu, HI. 3-5 Jan. 2001. ASAE, St. Joseph, MI.
- Maosheng, G., W. Pute, Z. Delan and Z. Lin (2018). Analysis of kinetic energy distribution of big gun sprinkler applied to continuous moving hose-drawn traveler. *Agricultural water management*, 201: 118-132.
- Melvyn, K., (1983). Sprinkler irrigation, equipment and practice. Batsford Academic and Educational, London, Pp.120.
- Muhaimeed, A. S., A. J. Saloom, K. A. Saliem, K. A. Alani and W. M. Muklef (2014). Classification and distribution of Iraqi soils. *Int. J Agric. Innov. Res.*, 2(6): 997-1002.
- Nolte, D. D. (2018). A Path Across Life, the Universe and Everything Oxford University Press. Galileo Unbound, pp. 39-63.
- Santos, F. L., J. L. Reis, O. C. Martins, (2003). Comparative assessment of infiltration, runoff and erosion of sprinkler irrigated soils. *Biosystems Engineering*, 86 (3): 355-364.
- Sayed D. M. (2016). Effect of some Engineering Factors of Sprinkler Irrigation on Sprinkler Performance, M.Sc., Thesis, Ain Shams Univ., pp. 21-22
- Sheikhesmaeili, O., Montero, J., Laserna, S., (2016). Analysis of water application with semi-portable big size sprinkler irrigation systems in semi-arid areas. *Agric. Water Manage.* 163, 275–284.
- Stillmunkes, R. T. and L. James (1982). Impact energy of water droplets from irrigation sprinklers. *Transactions of the ASAE*, 25 (1): 130-0133.

- Wang, Y., F. Yang, S. Qi and J. Cheng (2020). Estimating the effect of rain splash on soil particle transport by using a modified model. *Water*, 12(9): 23-18.
- Wang, Z., Y. Jiang, J. Liu and H. Li (2022). "Experimental Study on Water Distribution and Droplet Kinetic Energy Intensity from Non-Circular Nozzles with Different Aspect Ratios. *Agriculture*, 12(12): 21-33.
- Zhang, Y. and D. Zhu (2017). "Influence of sprinkler irrigation droplet diameter, application intensity and specific power on flower damage." *Frontiers of Agricultural Science Engineering*, 4(2): 165-171.

تأثير بعض المتغيرات الهندسية للرشاش التصادمي على معدل الأداء والطاقة الحركية للقطرات

سالي أحمد أمين^١، محمود محمد حجازي^٢، عبد الحميد توفيق جاب الله^٣ و خالد فران الباجوري^٤

^١ طالب دكتوراه- قسم كيمياء وطبيعة الاراضى – مركز بحوث الصحراء- القاهرة – مصر

^٢ أستاذ متفرغ - قسم الهندسة الزراعية – كلية الزراعة - جامعة عين شمس- مصر

^٣ أستاذ باحث متفرغ – قسم كيمياء وطبيعة الأراضى – مركز بحوث الصحراء- القاهرة – مصر

^٤ أستاذ - قسم الهندسة الزراعية – كلية الزراعة - جامعة عين شمس- مصر

الملخص العربي

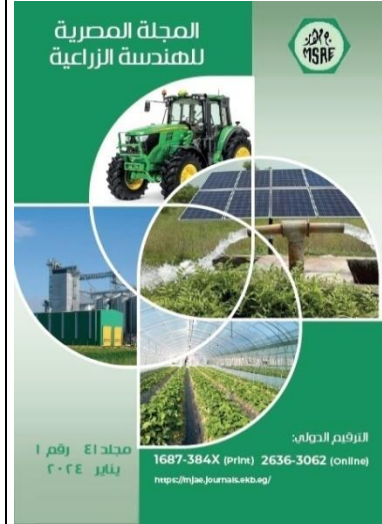
يهدف هذا البحث إلى الحصول على إدارة مناسبة للرشاشات التصادمية من أجل التغلب على مشكلة تلف الطبقة السطحية للتربة بسبب الطاقة الحركية للقطرات. كان لضغط المياه عند الفوهة وقطرها تأثير كبير على حجم القطرة مما يؤثر بشكل كبير على الطاقة الحركية للقطرة.

تم إجراء التجارب في المختبر القومي للري التابع لمعهد بحوث الهندسة الزراعية (AENRI)، الدقي، الجيزة، مصر لتمثيل البيانات الهندسية للرشاش التصادمي.

تم فحص فوهتين مختلفتين بقطر ٣,٢ مم و ٣,٩ مم في هذا العمل عند ثلاثة نطاقات مختلفة للضغط: ١٧٥ كيلو باسكال (٢٥,٤ رطل / بوصة مربعة) و ٢٠٠ كيلو باسكال (٢٩ رطل / بوصة مربعة) و ٢٢٥ كيلو باسكال (٣٢,٦ رطل / بوصة مربعة) ثم وجدنا النتائج على النحو التالي:

- معدلات الترسيب عند ضغط ٢٢٥ كيلو باسكال هي الأكثر انتظاماً، يليها ضغط ٢٠٠ كيلو باسكال يليه ضغط ١٧٥ كيلو باسكال للفوهتين المختبرتين.

- الطاقة الحركية للقطرة عند نهاية قطر الابتلال عند قطر الفوهة ٣,٢ مم تساوى (٢٦,٨٣ × ١٠^{-٣} جول)، (٢٣,٩ × ١٠^{-٣} جول) و (١٨,٣ × ١٠^{-٣} جول) عند ضغط ١٧٥ كيلو باسكال و ٢٠٠ كيلو باسكال و ٢٢٥ كيلو باسكال على التوالي، و عند قطر الفوهة ٣,٩ مم تساوي (٣٧,٧ × ١٠^{-٣} جول)، (٣٥,٧٨ × ١٠^{-٣} جول) و (٢٧,٨٢ × ١٠^{-٣} جول) عند ضغط ١٧٥ كيلو باسكال و ٢٠٠ كيلو باسكال و ٢٢٥ كيلو باسكال على التوالي.



© المجلة المصرية للهندسة الزراعية

الكلمات المفتاحية:

الرشاشات؛ الفوهات؛ الطاقة الحركية؛ معدل الترسيب؛ حجم القطرات.